Achromatic phase elements based on a combination of surface and volume diffractive gratings

Ivan Divliansky*, Evan Hale, Marc SeGall, Daniel Ott, Boris Y. Zeldovich, Bahaa E. A. Saleh, and Leonid Glebov
The College of Optics & Photonics, University of Central Florida
*ibd1@creol.ucf.edu

Abstract: Phase masks are important optical elements that have been utilized for several decades in a large variety of applications. Recently, we demonstrated a new type of phase masks fabricated by encoding phase profiles into volume Bragg gratings, allowing these holographic elements to be used as phase masks at any wavelength capable of satisfying the Bragg condition of the hologram. Here, we present a new method of true achromatization of this type of phase masks that removes the need for angle tuning and is implemented by combining this holographic phase masks approach with a pair of surface diffraction gratings.

Keywords: Achromatization, phase mask, volume hologram, volume Bragg gratings

Introduction

Optical phase masks have been used for various applications like encryption, beam shaping, mode conversion, and imaging based on the physical phenomenon of interference. The most common approach of making phase masks is based on varying the optical path length in certain areas of the phase mask. In order to produce the changes in path length, manufactures would generate a contoured surface in an optical material or generate a change in refractive index in photosensitive material. Consequently, since these phase shifts are based on changing optical path length the elements are only effective for a specifically designed wavelength. Previously we showed that it was possible and effective to encode stepped phase masks into transmitting Bragg gratings in photo-thermo-refractive (PTR) glass [1]. These holographic phase masks (HPMs) can successfully give a phase shift and achieve high diffraction efficiency (based on wavelength and the grating strength) for a broad range of wavelengths by tuning the element to the gratings Bragg condition for each discrete wavelength. In order to truly achromatize the HPM we present here an approach using the combination of surface diffraction gratings with a HPM to dispose of the need for angle tuning. In this paper we demonstrate the performance of a HPM paired with surface gratings as achromatic phase element for successful mode conversion over a range of 300nm.

Theory of Encoded Phase Masks

To encode the phase profile into a TBG, consider the recording setup in Fig. 1. Here a phase mask has been placed into one arm of a two-beam interference system, where the two beams interfere at an angle θ relative to the sample normal. The two-beam interference equation describing the fringe pattern in the sample will then be

$$I = I_1 + I_2 + 2\sqrt{I_1 I_2}\cos\left(\left(\vec{k}_1 - \vec{k}_2\right)\cdot\vec{r} + \varphi\left(x_0, y\right)\right), \quad (1)$$

where I is the intensity, $\vec{k}_i$ is the wavevector for each beam, and φ is the phase variation introduced by the phase mask after the object beam has propagated to the recording sample. If the thickness of the sample, the axial distance between the phase mask and the sample, and θ are small then $\varphi(x_0, y) \approx \varphi(x, y)$. The recorded TBG will therefore have a refractive index profile of $n(x, y, z) = n_0 + n_1\cos\left(\vec{K}\cdot\vec{r} + \varphi(x, y)\right)$, where n_0 is the background refractive index, n_1 is the refractive index modulation, and $\vec{K} = \vec{k}_1 - \vec{k}_2$ is the grating vector.

For a probe beam incident on the recorded hologram at or near the Bragg condition, the total electric field will satisfy the scalar Helmholtz wave equation,

$$\nabla^2 E - k_p^2 n^2 E = 0. \quad (2)$$

Components and Packaging for Laser Systems, edited by Alexei L. Glebov, Paul O. Leisher, Proc. of SPIE
Vol. 9346, 93460Q · © 2015 SPIE · CCC code: 0277-786X/15/$18 · doi: 10.1117/12.2081006

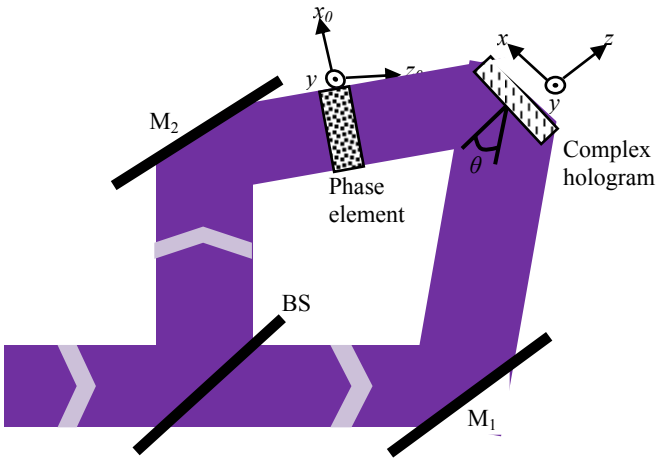

Fig. 1: Holographic recording of a phase mask.

Here k_p is the wavenumber of the probe beam. The Helmholtz equation has a general solution of the form [2]

$$E(x,y,z) = A(x,y,z)\exp\left(-i\vec{k}_p \cdot \vec{r}\right) + B(x,y,z)\exp\left(-i\vec{k}_d \cdot \vec{r}\right), \tag{3}$$

where A is the complex amplitude of the transmitted wave, B is the complex amplitude of the diffracted wave, and $\vec{k}_d = \vec{k}_p - \vec{K}$ is the wavevector of the diffracted beam. Inserting Eq. 3 into Eq. 2 will create a set of coupled wave equations between the amplitudes A and B. Kogelnik has solved these equations when A and B depend solely on the axial distance z [2], but because the phase term is not a constant when a phase mask is placed in the recording system it cannot be assumed that this one-dimensional dependence will still hold. For simplicity we will assume that the probe beam exactly satisfies the Bragg condition, as this case is the case of most interest to us. The coupled wave equations therefore become

$$\begin{aligned} \frac{1}{k_p}\left(k_{p,x}\frac{\partial A}{\partial x} + k_{p,y}\frac{\partial A}{\partial y} + k_{p,z}\frac{\partial A}{\partial z}\right) &= -i\kappa e^{-i\varphi(x,y)}B \\ \frac{1}{k_p}\left(k_{d,x}\frac{\partial B}{\partial x} + k_{d,y}\frac{\partial B}{\partial y} + k_{d,z}\frac{\partial B}{\partial z}\right) &= -i\kappa e^{i\varphi(x,y)}A \end{aligned}. \tag{4}$$

Here $\kappa=\pi n_1/\lambda_0$ is the coupling coefficient of the grating. Note that we have assumed that the second derivatives are negligibly small in the same manner as in Ref. [2].

These coupled-wave equations cannot be solved analytically in the general case. To solve them numerically we will first convert Eq. 4 into Fourier space along the transverse dimensions, giving

$$\begin{aligned} \frac{2\pi i}{k_p}\left(f_x k_{p,x} + f_y k_{p,y}\right)\widetilde{A} + \frac{k_{p,z}}{k_p}\frac{\partial \widetilde{A}}{\partial z} &= F\left\{-i\kappa e^{-i\varphi(x,y)}B\right\} \\ \frac{2\pi i}{k_p}\left(f_x k_{d,x} + f_y k_{d,y}\right)\widetilde{B} + \frac{k_{d,z}}{k_p}\frac{\partial \widetilde{B}}{\partial z} &= F\left\{-i\kappa e^{i\varphi(x,y)}A\right\} \end{aligned}, \tag{5}$$

where $\tilde{A}$ is the Fourier transform of A and $\widetilde{B}$ is the Fourier transform of B. To solve these equations we will split the propagation and energy conservation into two discrete steps. To calculate the propagation of the beam assume that the right side of Eq. 5 equals zero. In this cased the amplitudes will have a solution of the form

$$\begin{aligned}\widetilde{A}\left(f_x, f_y, z+\Delta z\right) &= \widetilde{A}\left(f_x, f_y, z\right)\exp\left(-i\frac{2\pi}{k_{p,z}}\left(f_x k_{p,x}+f_y k_{p,y}\right)\Delta z\right)\\ \widetilde{B}\left(f_x, f_y, z+\Delta z\right) &= \widetilde{B}\left(f_x, f_y, z\right)\exp\left(-i\frac{2\pi}{k_{d,z}}\left(f_x k_{d,x}+f_y k_{d,y}\right)\Delta z\right)\end{aligned} \tag{6}$$

Note that this only exact in the case where the right side of Eq. 5 equals zero but for small (~100 nm) propagation steps this is a reasonable approximation. The amplitude in real space is therefore the inverse Fourier transform plus the left side
of Eq. 5:

$$\begin{aligned}A(x,y,z+\Delta z) &= F^{-1}\left\{\widetilde{A}\left(f_x, f_y, z+\Delta z\right)\right\} - i\kappa e^{-i\varphi(x,y)}B(x,y,z)\Delta z\\ B(x,y,z+\Delta z) &= F^{-1}\left\{\widetilde{B}\left(f_x, f_y, z+\Delta z\right)\right\} - i\kappa e^{i\varphi(x,y)}A(x,y,z)\Delta z\end{aligned} \tag{7}$$

Calculations indicate that for a propagation step size of 100 nm energy is conserved to within 0.01%, which is sufficient for the phase profiles discussed here.

To determine the diffracted beam profile and diffraction efficiency in the case where a binary phase profile is encoded we simulated a grating with an 8 μm period, a refractive index modulation of 250 ppm, and a thickness of 2 mm. For a homogenous transmitting Bragg grating and a probe beam wavelength of 1064 nm, the diffraction efficiency is 99.13%. If a binary step is introduced, where the binary step is at a recording wavelength of 325 nm, then the diffraction efficiency will decrease by up to a few percent depending on the probe beam diameter and the orientation of the phase discontinuity relative to the probe beam propagation vector. This decrease in diffraction efficiency is caused by the step discontinuity, where it is not possible to satisfy the Bragg condition at 1064 nm. However, regardless of the diffraction efficiency and orientation of the phase discontinuity, in all cases the diffracted beam had a binary phase profile at 1064 nm. Therefore, as the decrease in diffraction efficiency is largely negligible for beam diameters larger than 1 mm, we conclude that ideal binary phase masks encoded into TBGs will allow for reconstruction of the phase profile at any wavelength capable of satisfying the Bragg condition with effectively the same diffraction efficiency as homogenous gratings.

Holographic Phase Masks

The holographic phase mask proof of concept was presented in previous work [1], where holograms of a four-sector mode converting mask (chosen to give a binary phase shift along the horizontal and vertical axes in a single element) were recorded using a Mach-Zehnder-type recording system in 1.97 mm-thick photo-thermo-refractive (PTR) glass (Fig. 1) [3].

The holographic phase mask was examined in the far field (achieved by focusing the beam with a 500 mm lens) at multiple wavelengths in the visible and the infrared regions using a 3 mm probe beam to determine the wavelength dependence of mode conversion. As shown in Fig. 2, in all cases the diffracted profile exhibited the same four-lobed pattern. The profiles in Fig. 2 are very similar to the far field profile of the four-sector standard volume phase mask in [4], indicating that there is a phase dependence encoded into the volume grating.

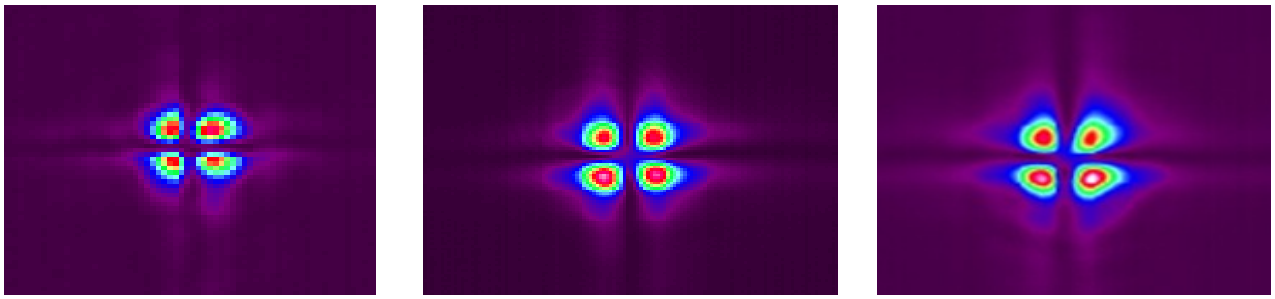

(a) (b) (c)

Fig. 2: Far field profile of the diffracted beam after propagating through a holographic four-sector mode converting mask at (a) 632.8 nm, (b) 975 nm, and (c) 1064 nm. The sizes shown here are not to scale.

The mode converting ability of the phase masks is of course not limited to converting a Gaussian beam to a higher order mode; it is also possible to convert from a higher order mode to a Gaussian profile. To demonstrate this, two 4-sector mode converting holographic phase masks were aligned so that a 3 mm Gaussian beam at 1064 nm was incident on the first mask and the diffracted (converted) beam from this mask was incident on the second converter. This doubly converted beam was then focused by a 500 mm lens to achieve the far field profile. As shown in Fig. 3a, the far field profile is a Gaussian spot with some low-energy side lobes. Cross sections of the beam, shown in Fig. 3b and 3c, were fitted with Gaussian functions to determine the size of the main spot relative to a diffraction-limited spot. The fits indicate that the spot size along the horizontal axis is 228 µm, nearly identical to the diffraction-limited spot size of 226 µm, while the spot size along the vertical axis is 240 µm, which is close to diffraction-limited. The wings are caused by the finite transition regions at the boundary between the different grating phases and can be reduced by reducing the size of the transition regions in the original phase mask used for recording as well as placing the phase mask closer to the sample during recording.

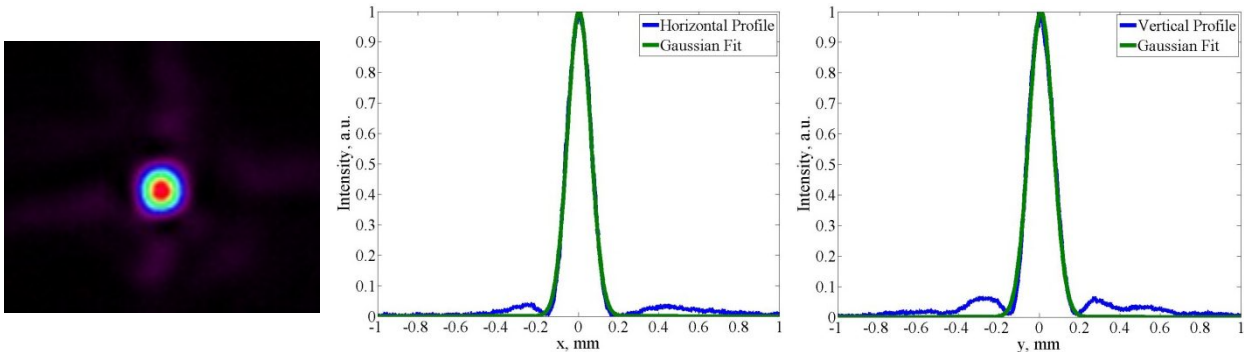

(a) (b) (c)

Fig. 3: (a) Far field profile of a beam converted from a higher order mode to a Gaussian profile. (b) Horizontal and (c) vertical cross sections of the beam indicate that the central spot is nearly diffraction limited.

The diffraction efficiency of these volume phase masks can be compared to a homogenous grating by multiplexing a homogenous grating and volume phase mask in a single element. This was done by recording a volume phase mask in the setup shown in Fig. 1 and then removing the phase mask in the object beam and rotating the PTR sample to record a homogenous grating. As shown in Fig. 4, the diffraction efficiencies of each element are approximately the same, showing good agreement with theoretical predictions.

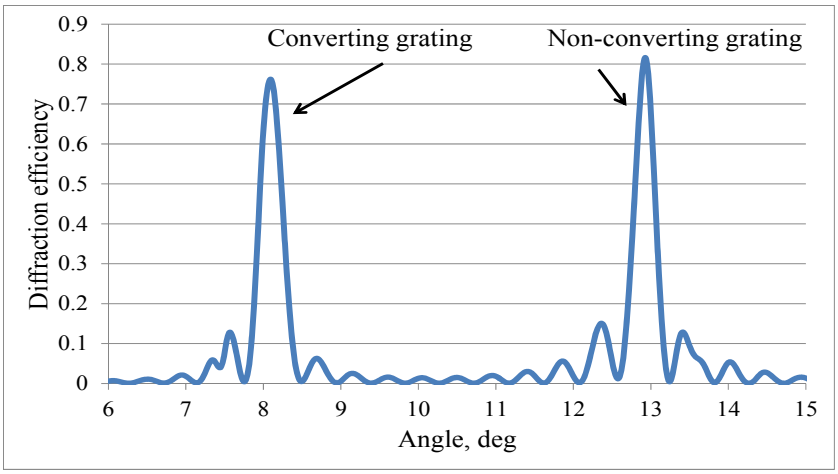

Fig. 4: Diffraction efficiency of a volume phase mask converting a Gaussian beam to the TEM_{11} mode compared to the diffraction efficiency of a homogenous grating.

Achromatization with Surface Diffraction Gratings

True achromatization of HPMs can be achieved with the concept of pairing the Bragg grating with two surface gratings [5]. According to the grating dispersion equation (Eq. 8), a surface grating with a given period (Λ_{SG}) will diffract normally incident light an angle (θ) in different orders as a function of wavelength (λ).

$$\Lambda_{SG} \sin\theta = m\lambda \tag{8}$$

As well, based on coupled wave theory [2], a VBG will diffract light highly efficient at the Bragg condition Eq. 9. Under this condition light is incident and diffracted at the Bragg angle (θ_B), and diffraction efficiencies for these gratings can be as efficient as 100% [2].

$$2\Lambda_{VBG} \sin\theta_B = \lambda \tag{9}$$

$$2\Lambda_{VBG} = \Lambda_{SG} \tag{10}$$

Since both of these diffraction angles are dependent on the grating period, theoretically if the surface grating period is double the period (Eq. 10) of the volume Bragg grating then any first order diffraction by normally incident light will be at the corresponding Bragg condition of the volume Bragg grating and that will hold for any wavelength [5]. If we add an identical surface grating in a mirror orientation to the transmitting volume Bragg grating like shown in Fig. 5, we can completely cancel out the dispersion and re-collimate the outgoing beam . Applying this concept to our holographic phase mask the need for angle tuning to the Bragg condition can be disregarded, making it a fully achromatic phase element.

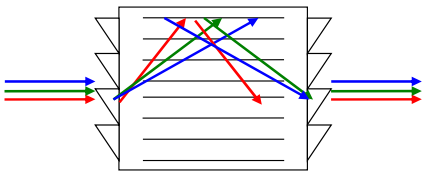

Fig. 5: Concept of using surface gratings pairs to meet the Bragg condition for various wavelengths regardless of angle tuning [5].

As proof of concept, two surface gratings with a grove spacing of 150 lines/mm (a period of 6.66 µm) were aligned to a HPM with a period of 3.4µm in our experimental set up shown in Fig 6. The goal of our experiment was to

achieve successful broadband mode conversion from a Gaussian to a TEM_{11} mode without the need to angularly tune the HPM. In our experiment three different tunable diode laser sources were used in order to get a wavelength range of over 300 nm (765-1071 nm). The lasers were collimated individually with a 6 mm collimator in order to unsure full illumination of the HPM. The first surface grating was aligned so that the HPM's Bragg condition would be met for all wavelengths, and then the second grating was placed to nullify the beam deviation and dispersion. Surface gratings with a blaze wavelength of 725 nm were chosen with diffraction efficiencies in the range of 50% to 70% for the corresponding 765-1071 nm spectral range. To achieve far field imaging, the beam was focused on a CCD camera with an achromatic lens (f=500 mm).

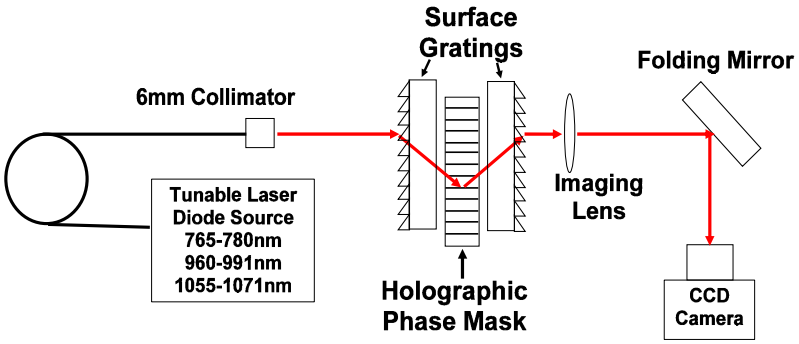

Fig. 6: Experimental set up for observing Gaussian to TEM_{11} conversion of the HPM surface grating system with three different diode sources.

Fig. 7 demonstrates the TEM_{11} mode profile for a single wavelength for each one of the three laser sources. The differences in the intensities are due to the difference in output power for each of the diode sources. Figure 7 also demonstrates that HPMs can provide the same quality phase transformation as regular phase masks with the main difference being that one HPM works for very broad spectral range, as demonstrated.

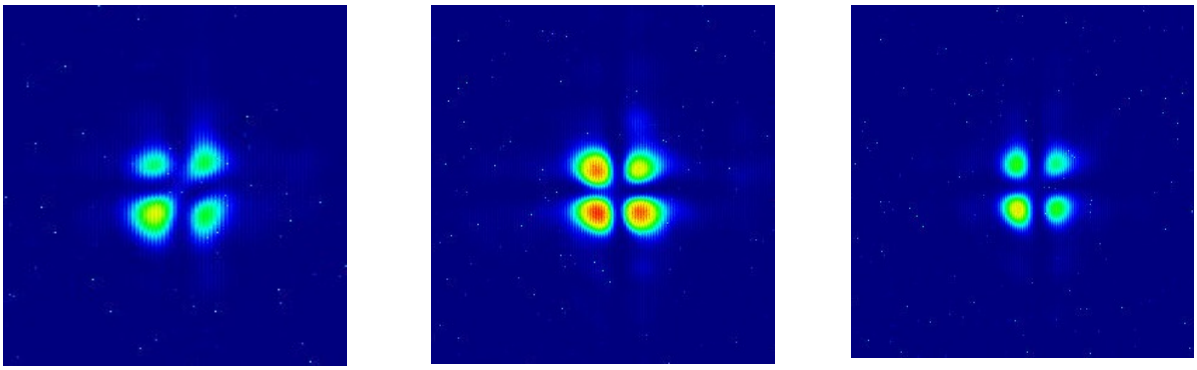

(a) (b) (c)

Fig. 7: Far field profile of the diffracted beam after propagating through a holographic four-sector mode converting mask aligned to two surface gratings at (a) 765 nm, (b) 978 nm, and (c) 1071 nm. The sizes shown here are not to scale.

Three different experiments were done based on the combination of the gratings used and are presented in Fig 8. The first experiment had the two surface gratings removed, and Fig. 8(a) shows only images of the beam after the HPM (no surface diffraction gratings present on its sides). The wavelength bandwidth of the HPM is limited to the bandwidth of a transmission Bragg grating and therefore it can only diffract in this particular case approximately 12 nm without angular adjustment. Because of this the top picture in Fig. 8(a) does not show any signal after for wavelengths less than 1056 nm and larger than 1066 nm. In the second experiment, from which results are shown in Fig. 8(b), we introduced the one surface diffraction grating on the left side of the HPM. For this configuration, the bandwidth of the system is dramatically increased and maximum diffraction efficiency (and therefore mode conversion) is being achieved

for wider spectral region. However, due to the wavelength dispersion of the surface grating the signal walks off the camera. To nullify the lateral movement of the beam present in this second experiment, a second surface grating was added and the images for a scan of over 300 nm are shown in Fig. 8(c). Fig. 8(c), clearly proves that the combination of two surface gratings and a holographic phase plate with accordingly matched periods works as achromatic phase element over very wide wavelength region.

Since we used three different tunable laser sources and for each one the 6 mm collimator had to be realigned a beam hopping is observed when switching between the three spectral regions covered in column (c). Some small beam shifting is also present while sweeping each of the individual sources. We attribute this effect to the non-exact ratio between the TBG and the surface gratings periods.

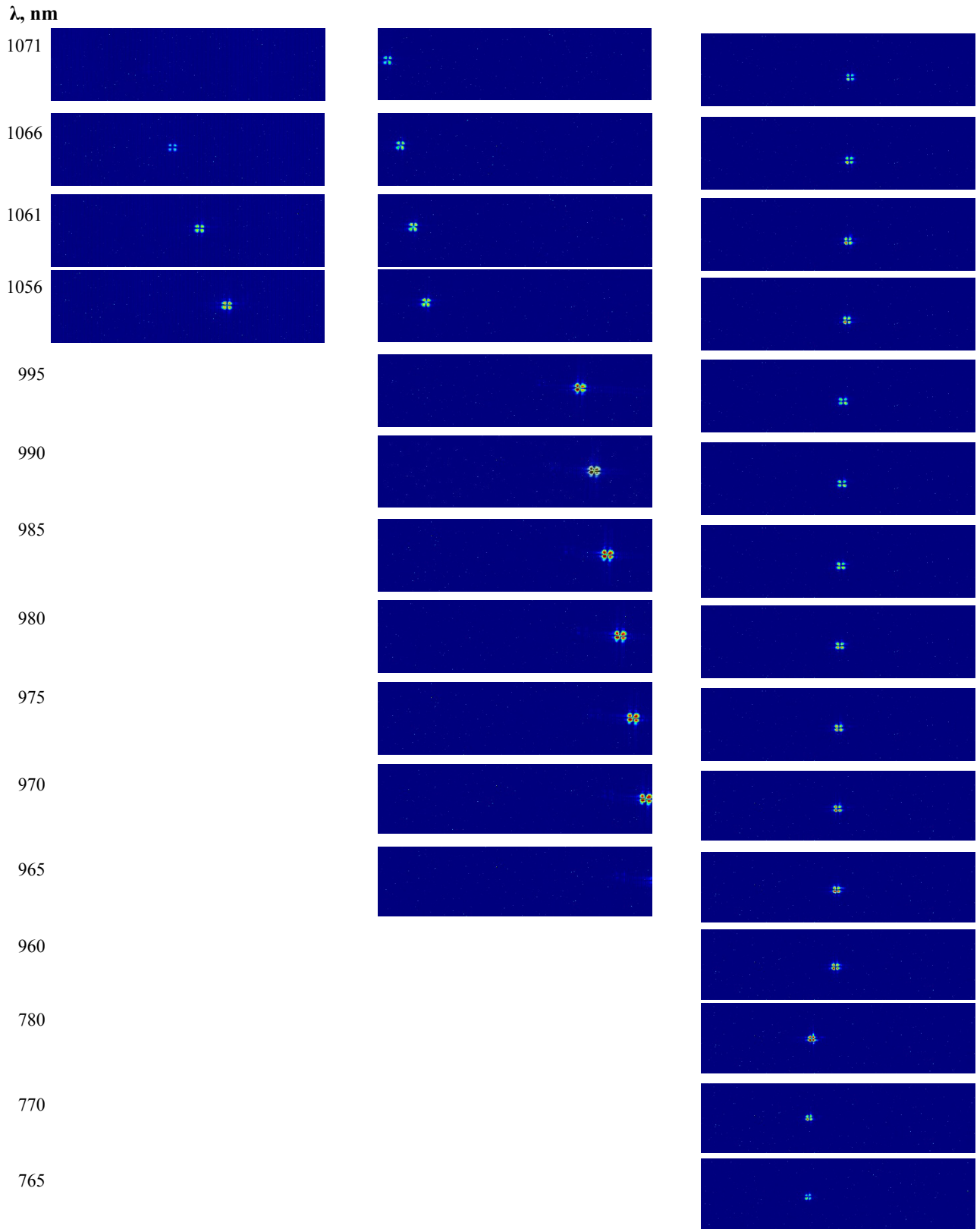

Fig. 8: Far field profiles of the diffracted beam after propagating through (a) a holographic four-sector mode converting mask, (b) one surface grating aligned to the Bragg angle of a holographic mask, and (c) two surface gratings aligned to the Bragg angle of a holographic phase mask.

Conclusions

We have successfully demonstrated that full achromatization of a holographic phase mask can be achieved with the combination of surface gratings and phase encoded transmitting volume Bragg grating. An experimental mode conversion from a Gaussian to a TEM_{11} mode for a range of more than 300 nm was successfully achieved with a single phase element and without any angular adjustments.

This work is supported by the HEL JTO and ARO through grant No. W911NF-10-1-0441.

References

1. SeGall, M., Divliansky, I., Jollivet, C., Schülzgen, A., Glebov, L., "Simultaneous laser beam combining and mode conversion using multiple volume phase elements," Proceedings of SPIE 896050 (2013).
2. Kogelnik, H., "Coupled wave theory for thick volume holograms," Bell System Tech. J. 45, 2909-2944 (1969).
3. Glebov, L. "Photosensitive glass for phase hologram recording," Glass Sci. Technol. 71, 85-90 (1998).
4. SeGall, M., Rotar, V., Lumeau, J., Mokhov, S., Zeldovich, B., and Glebov, L., "Binary volume phase masks in photo-thermo-refractive glass," Opt. Lett. 37, 1190-1192 (2012).
5. L. Glebov, V. Smirnov, N. Tabirian and B. Zeldovich, "Implementation of 3D Angular Selective Achromatic Diffraction Optical Grating device", Frontiers in Optics 2003, Talk WW3.